Electronic Supplementary Material (ESI) for RSC Advances.

ELECTRONIC SUPPLEMENTARY INFORMATION

Development of small-volume, microfluidic chaotic mixers for future application in two-dimensional liquid chromatography

Margaryta A. Ianovska,[a,b] Patty P.M.F.A. Mulder,[a] Elisabeth Verpoorte[a]

[a] Pharmaceutical Analysis, Groningen Research Institute of Pharmacy, University of Groningen, Antonius Deusinglaan 1, P.O. Box 196, 9713 AV Groningen, The Netherlands.

[b] TI-COAST, Science Park 904, 1098 XH Amsterdam, THE NETHERLANDS

* Corresponding author.

E-mail address: E.M.J.Verpoorte@RuG.nl

Tel: +31 50 363 3337

Fax: +31 50 363 7582

Table of contents:

S-1 CHEMICALS AND REAGENTS

All chemicals were analytical reagent-grade. Fluorescein was purchased from Sigma-Aldrich (NL) and used to prepare separate 5.0 µM fluorescein solutions in 10.0 mM phosphate-buffered saline with pH 7.4 (PBS; Gibco, UK). Acetonitrile (HPLC-S) and methanol were both obtained from Biosolve, The Netherlands. The pH was measured using pH-indicator strips (Neutralit, MERCK). All solutions were prepared with 18 M-ohm ultrapure water (Arium 611, Sartorius Stedim Biotech, Germany). Both acetonitrile and methanol were degassed for 15 min prior to experiments.

S-2 CHIP FABRICATION AND ASSEMBLY

The microchannels were constructed by standard microfabrication and replicated in the silicone rubber, poly(dimethylsiloxane)(PDMS)(Sylgard 184, Dow Corning, U.S.). The chip layout and design were drawn using the software Clewin (Wieweb software, Hengelo, The Netherlands).

Masters were fabricated using two steps of standard photolithography in the negative photoresists SU-8 50 and SU-8 10 (MicroChem). These resists were optimized for different layer thicknesses (SU-8 50 was used to pattern microchannels, and SU-8 10 to pattern the grooves) (Figure S-1A). The conditions were chosen based on the recommended parameters described by MicroChem, the manufacturer of SU-8 photoresists.[1,2]

A 4-inch borofloat wafer (700 µm thickness, Borofloat 33, Handelsagentur Helmut Teller, Jena, Germany) was employed as a substrate. The wafer was cleaned sequentially with acetone, isopropyl alcohol, and ultrapure water, dried with N_2 gas and baked for 5 min at 150°C to remove residual water. A first layer of negative photoresist (PR), SU-8 50 (MicroChem, Newton, MA), was coated on the wafer using 500 rpm for 13 sec followed by different speeds, depending on the required layer thickness (Table S-1). The wafers were then soft-baked (from 20°C to 65°C in 45 min, 8 min at 65°C, from 65°C to 95°C in 30 min, 25 min at 95°C and cooled down to room temperature on the hotplate). The coated wafer was illuminated with ultraviolet (UV) light (365 nm, 10 mW/cm^2) from a collimated light source to pattern the microchannels, using a photomask printed on a transparency (resolution 3,810 dpi; Pro-

Art BV, Groningen, The Netherlands). The illumination was followed by a post-bake step (from 20°C to 65°C in 45 min, 1 min at 65°C, from 65°C to 95°C in 30 min, 8 min at 95°C and cooled down to room temperature).

Wafers were then exposed to oxygen plasma (Harrick plasma, USA) to ensure adhesion of the second photoresist layer for 20 sec. The second layer of SU-8 10 photoresist was spin-coated with SU-8 10 (MicroChem, Newton, MA) at different speeds, depending on the required layer thickness (Table S-1), soft-baked at the conditions mentioned above and illuminated by UV light. The second photomask, which contains the pattern for grooves only, was aligned manually with the microchannels in the first layer under the microscope using alignment marks. After the post-bake step, wafers were immersed in SU-8 developer for 15 min, rinsed with isopropanol and dried using N_2 gas. They were then placed under vacuum in the presence of hexamethyldisilazane (HMDS) (Sigma-Aldrich, Germany) for at least 30 min to make the wafer surface more hydrophobic and thus facilitate the peeling of the cured PDMSfrom the masters. The heights of the channels and grooves on the masters were determined using a profilometer (Veeco Instrument BV, located in the Zernike NanoLab Groningen, The Netherlands).

Table S-1. Spin coating conditions for different photoresist layer thickness.

1st layer (SU-8 50)		**2nd layer (SU-8 10)**	
Speed, rpm	Layer thickness, µm	Speed, rpm	Layer thickness, µm
1600 (40 sec)	60	750 (30 sec)	50
1300 (40 sec)	80	1300 (35 sec)	30
1300 (35 sec)	90	1500 (45 sec)	20

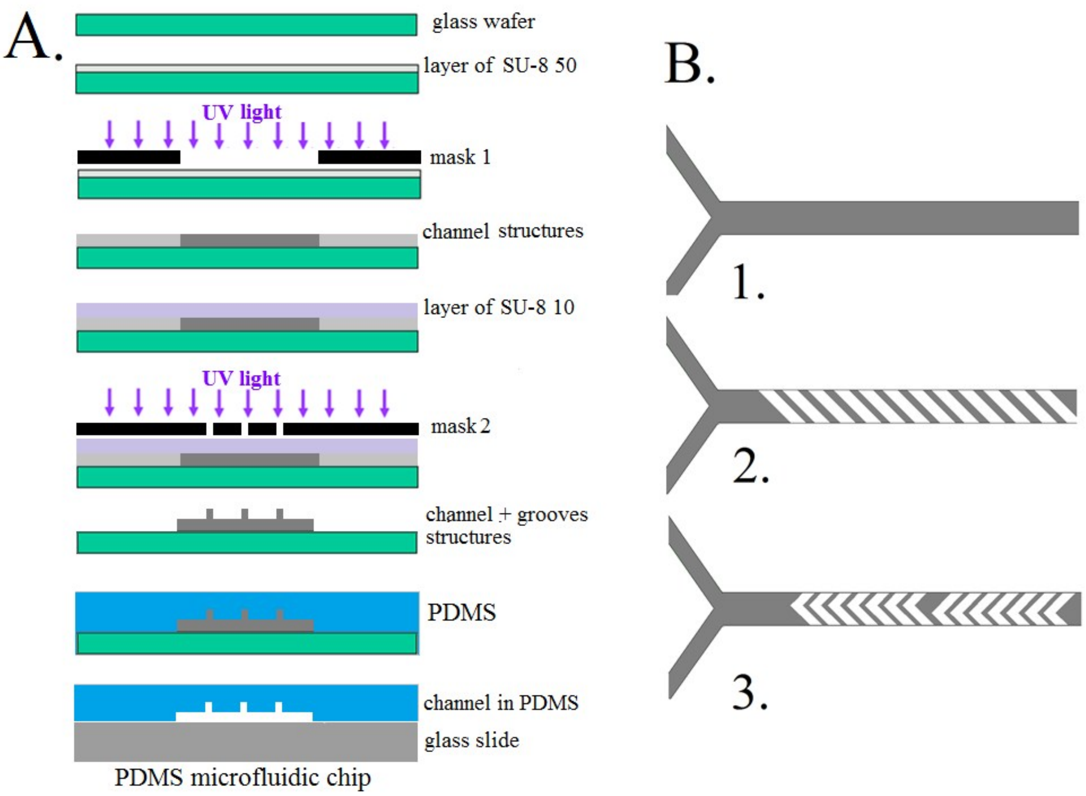

Figure S-1. (A) A schematic diagram of the two-step photolithography fabrication process. **(B)** Schematic drawing (top view) of the three types of channels investigated in this study: channel without grooves (1); channel with slanted grooves (2); channel with herringbone grooves (3).

S-3 INVESTIGATION THE MIXING MECHANISM

Evaluation of the degree of mixing by conventional microscopy in the manner that we have done may yield misleading data with respect to mixing in microchannels. Image analysis for our reported experiments was done using top-view images of the channel. However, during mixing, fluids change their orientations inside the channel, and fluid zones containing different dye concentrations can be situated perpendicular or parallel to the camera of the microscope. This means that an observed equal distribution of fluorescence for the channel top-view may not necessarily correspond to complete mixing. In order to confirm the reliability of of our image analysis, and at the same time investigate the mixing mechanism at the cross-sections of the mixing channel, we utilized confocal microscopy.

Figure S-2 shows the cross sections of the HG mixer at positions from 0 to 9.5 mm along the channel obtained by confocal microscopy. The first image (position 0 mm) shows two fluids, PBS and PBS-fluorescein, flowing in the channel before entering the region with grooves. The second image represents the situation where the solution from the left inlet hits the sharp edge of the groove and a portion of the solution moves along the long groove arm. At this point the flow from the left inlet splits into two parts, as was reported previously by Yang *et al.*[3] One part of the flow moves further to the right side, enters the groove and hits the next rigid curve backwards, which results in formation of the counterclockwise-rotating vortex. Another part of the flow rolls out of the groove on the left side and returns to the mainstream. This process results in clockwise rotation. On the images obtained with confocal microscopy (Fig. S-2) the generation of two counter-rotating asymmetrical vortices can be clearly observed. These vortices change in asymmetry from one half-cycle to another. For this micromixer with a groove width, *a*, of 80 μm and channel width, *w*, of 300 μm, grooves start at 0.78 mm and one full cycle occupies 2.0 mm (each half-cycle is 0.98 mm plus interval between half-cycles). Therefore, there are 21 full cycles within the 50 mm channel length. Moving from a position of 2.3 mm (Fig. S-2.B), which indicates the first half-cycle, to a position of 3.2 mm, which indicates the second half-cycle, we clearly see two counter-rotating vortices with changed asymmetry in between half-cycles. These results are in good agreement with both the numerical simulations [3–5] and experimental results by Stroock *et al.* [6,7]

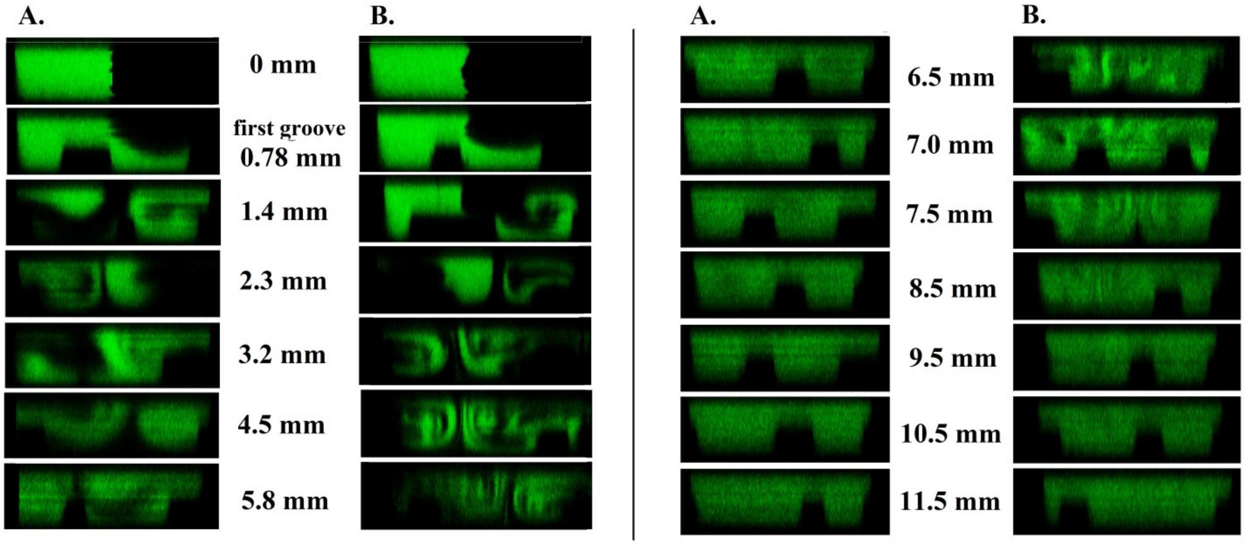

Figure S-2. Images of the cross sections of the HG mixer obtained using confocal microscopy at total flow rate **(A)** 20 µL/min (*Pe* ~ 5×10^3, Re 1.6) and **(B)** 200 µL/min (*Pe* ~ 50×10^3, Re 16.3); distance from the Y-junction: 0 - 11.5 mm of the channel length; w = 300 µm; a = 80 µm; PBS (fluorescein)-PBS 1:1. Mixing is facilitated by the generation of two counter-rotating asymmetrical vortices. Equal distribution of fluorescein on the images indicates the complete mixing.

Yang *et al.* [3] identified two dominant mechanisms of mixing in the HG mixer: (1) the stretching and folding of the interface due to the vertical motions of flow at the side edge of the groove and (2) the increase in contact area between the two fluids due to fluid transportation inside the groove. Stretching and folding are chaotic processes that lead to the production of chaotic advection.[8] The flow velocity components are constant over space and time in chaotic advection, in contrast to the turbulent flow where these are considered to be random.[4]

Experiments were carried out using two flow rates: 20 µL/min (Fig. S-2A) and 200 µL/min (Fig. S-2B). It is reasonable to expect that mixing should be achieved faster at the lower flow rate. The influence of the flow rate on the behavior of mixing can be clearly observed. Compared with the smooth vortices (due to longer residence time) at lower flow rate (Fig. S-2A), the high flow rate introduces agitation to the flows creating more chaotic flow patterns and increasing the contact area between them. Such effects are what make the HG mixer efficient over the wide range of flow rates tested. As the flow rate increases by a factor of 10 (from 20 to 200 µL/min), the distance required for complete mixing increases only by a factor of 1.35 (from 7.0 to 9.5 mm). These results are in good accordance with our previous data (Figure 3) obtained by fluorescence microscopy, where we showed that 10 mm was enough to complete mixing at *Pe* < 10^5.

S3 REFERENCES

1 *Brochure provided by NANO^{TM} SU-8 Negative Tone Photoresist Formulations 50-100* .

2 *Brochure provided by NANO^{TM} SU-8 Negative Tone Photoresist Formulations 2-25*.

3 J.-T. Yang, K.-J. Huang and Y.-C. Lin, *Lab Chip*, 2005, **5**, 1140.

4 E. Tóth, E. Holczer, K. Iván and P. Fürjes, *Micromachines*, 2014, **6**, 136–150.

5 J. Aubin, D. F. Fletcher, J. Bertrand and C. Xuereb, *Chem. Eng. Technol.*, 2003, **26**, 1262–1270.

6 A. D. Stroock, S. K. W. Dertinger, A. Ajdari, I. Mezic, H. a Stone and G. M. Whitesides, *Science*, 2002, **295**, 647–51.

7 A. D. Stroock and G. M. Whitesides, *Acc. Chem. Res.*, 2003, **36**, 597–604.

8 N.-T. Nguyen , *Micromixers: Fundamentals, Design and Fabrication,* William Andrew Publishing, Norwich, NY, USA, 2011.